Nongenomic Effects of Fluticasone Propionate and Budesonide on Human Airway Anion Secretion

Takefumi Mizutani[1], Masahiro Morise[1], Yasushi Ito[1], Yoshitaka Hibino[1], Tadakatsu Matsuno[1], Satoru Ito[1], Naozumi Hashimoto[1], Mitsuo Sato[1], Masashi Kondo[1], Kazuyoshi Imaizumi[1], and Yoshinori Hasegawa[1]

[1]Department of Respiratory Medicine, Nagoya University Graduate School of Medicine, Nagoya, Japan

This study investigated the physiological effects of inhaled corticosteroids, which are used widely to treat asthma. The application of fluticasone propionate (FP, 100 μM) induced sustained increases in the short-circuit current (I_{SC}) in human airway Calu-3 epithelial cells. The FP-induced I_{SC} was prevented by the presence of H89 (10 μM, a protein kinase A inhibitor) and SQ22536 (100 μM, an adenylate cyclase inhibitor). The FP-induced responses involved bumetanide (a Na^+–K^+–$2Cl^-$ cotransporter inhibitor)–sensitive and 4,4′-dinitrostilbene-2,2′-disulfonic acid (an inhibitor of HCO_3^--dependent anion transporters)–sensitive components, both of which reflect basolateral anion transport. Further, FP augmented apical membrane Cl^- current (I_{Cl}), reflecting cystic fibrosis transmembrane conductance regulator (CFTR)–mediated conductance, in the nystatin-permeabilized monolayer. In I_{SC} and I_{Cl} responses, FP failed to enhance the responses to forskolin (10 μM, an adenylate cyclase activator). Nevertheless, we found that FP synergistically increased cytosolic cAMP concentrations in combination with forskolin. All these effects of FP were reproduced with the use of budesonide. Collectively, inhaled corticosteroids such as FP and budesonide stimulate CFTR-mediated anion transport through adenylate cyclase–mediated mechanisms in a nongenomic fashion, thus sharing elements of a common pathway with forskolin. However, the corticosteroids cooperate with forskolin for synergistic cAMP production, suggesting that the corticosteroids and forskolin do not compete with each other to exert their effects on adenylate cyclase. Considering that such synergism was also observed in the FP/salmeterol combination, these nongenomic aspects may play therapeutic roles in mucus congestive airway diseases, in addition to genomic aspects that are generally recognized.

Keywords: fluticasone propionate; budesonide; cAMP; anion transporter; forskolin

Inhaled corticosteroids are well-established anti-inflammatory therapies for the prophylactic treatment of asthma, and are recommended in national treatment guidelines as first-line therapy in persistent asthma (1). Beclomethasone dipropionate has been in use for almost 30 years as an inhaled asthma medication (2). In the 1990s, fluticasone propionate (FP) and budesonide, with more potent anti-inflammatory effects than beclomethasone dipropionate, were introduced and remain the drugs of first choice (3, 4). In general, anti-inflammatory effects of corticosteroids are well recognized to depend on the classic steroid receptors (5). Their effects involve a complex process, including ligand-receptor binding in the cytosol, targeted gene expression, and protein synthesis, so that hours may pass before the onset of hormone actions (6). This is called the genomic mechanism. However, several lines of evidence have demonstrated that sex steroids and xenoestrogens also exert their effects via nongenomic mechanisms, which are acute in onset and require membrane steroidal receptors without the involvement of nuclear steroid receptors and gene expression (6). The rapid interaction leads to changes in the kinetics of ion channels such as K^+ channels (7, 8), L-type Ca^{2+} channels (9, 10), and Cl^- channels (11, 12) in various kinds of cells. Despite the evidence, however, less attention has been paid to the acute effects of inhaled corticosteroids on ion channels and transporters. Because steroids are applied directly to the apical side of the respiratory tract, higher concentrations of the drugs on the airway surface are supposed to be achieved than with intravenous application. It is generally established that anion transport mediated through the cystic fibrosis transmembrane conductance regulator (CFTR) anion channel is important in the formation of low-viscosity mucus, thereby maintaining a conductive and aseptic environment in the lung (13). Indeed, dysfunction of the CFTR, as seen in patients with cystic fibrosis, results in the production of thick mucus plugs and consequently causes serious respiratory damage (13). Thus, a potential strategy to combat airway obstructive diseases has involved exploring the pharmacological agents that up-regulate CFTR-mediated ion transport. In the present study, we focused especially on the nongenomic effects of inhaled corticosteroids on anion secretion in human airway epithelial cells.

CLINICAL RELEVANCE

We demonstrate that fluticasone propionate and budesonide stimulate cystic fibrosis transmembrane conductance regulator–mediated anion transport through adenylate cyclase–mediated mechanisms in a nongenomic fashion. The effects of the corticosteroids on adenylate cyclase synergistically enhance the production of cAMP, in combination with cAMP-related agents (e.g., forskolin and salmeterol). The nongenomic effects may involve therapeutic aspects for mucus congestive airway diseases, such as bronchial asthma and chronic obstructive pulmonary disease, in addition to genomic effects that are conventionally recognized.

MATERIALS AND METHODS

Chemicals

Forskolin, nystatin, 4,4′-dinitrostilbene-2,2′-disulfonic acid (DNDS), 5′-nitro-2-(3-phenylpropylamino)benzoate (NPPB), and 9-tetrahydro-2-furyl-adenine (SQ22536) were obtained from Sigma-Aldrich Co. (St. Louis, MO). Bumetanide and *N*-[2-(p-bromocinnamylamino)

(*Received in original form February 24, 2012 and in final form July 4, 2012*)

This work was supported by a grant from the Global Center of Excellence Program funded by the Ministry of Education, Culture, Sports, Science, and Technology of Japan.

Correspondence and requests for reprints should be addressed to Yasushi Ito, M.D., Ph.D., Department of Respiratory Medicine, Nagoya University Graduate School of Medicine, Nagoya 466-8550, Japan. E-mail: itoyasu@med.nagoya-u.ac.jp

This article has an online supplement, which is accessible from this issue's table of contents at www.atsjournals.org

Am J Respir Cell Mol Biol Vol 47, Iss. 5, pp 645–651, Nov 2012

Originally Published in Press as DOI: 10.1165/rcmb.2012-0076OC on July 12, 2012
Internet address: www.atsjournals.org

ethyl]-5-isoquinolinesulfonamide (H89) were purchased from Biomol International, LP (Plymouth Meeting, PA). FP and budesonide were products of Tocris Bioscience, Inc. (Ellisville, MO).

Cell Culture

Calu-3 human airway cells (American Type Culture Collection, Manassas, VA) were grown in a 1:1 mixture of Dulbecco's Modified Eagle's Medium and Ham's F-12 (Invitrogen, Carlsbad, CA) containing 10% FBS (Invitrogen), 100 μg/ml streptomycin, and 100 U/ml penicillin (Invitrogen). The cells were maintained in tissue-culture flasks (T75) at 37°C in a humidified 95% air–5% CO_2 incubator. After reaching 80 to 90% confluence, cells were detached using a solution of PBS, 0.04% EDTA, and 0.25% trypsin. The collected cells were seeded onto Snapwell inserts (Costar, Cambridge, MA) at a density of 10^6 cells/well. The inserts had been collagen-coated overnight with 0.2% human placental collagen Type VI (Sigma-Aldrich). The day after seeding the cells on the filters, the medium remaining on the apical side was removed to establish an air interface (14). The cells were fed by replacement of the basolateral medium every 48 hours. Experiments were performed after 7 to 13 days in culture (*see* additional details in the online supplement).

Bioelectric Measurements

Calu-3 cells were grown on Snapwell inserts, and were mounted in Ussing chambers filled with physiological saline solution containing 115 mM NaCl, 5 mM KCl, 1 mM $MgCl_2$ 2 mM $CaCl_2$, 10 mM glucose, 10 mM HEPES, and 25 mM $NaHCO_3$, whose pH was adjusted to 7.4 when gassed with a mixture of 95% O_2–5% CO_2 at 37°C for short-circuit current (I_{SC}) measurements, as previously described (15). I_{SC} changes were measured under voltage clamp conditions, using a voltage clamp amplifier (VCC MC2; Physiologic Instruments, San Diego, CA). A 2-mV pulse of 0.5-second duration was imposed every 20 seconds to calculate resistance by Ohm's law.

Apical membrane Cl^- currents (I_{Cl}) in the apical-to-basolateral Cl^- concentration gradient were estimated after permeabilization of the basolateral membrane with nystatin (100 μM), as previously described (15–17). The I_{Cl} reflects Cl^- permeability through the CFTR (18, 19). The Cl^- concentration gradient was established by replacing NaCl with equimolar Na-gluconate in the basolateral solution. In this basolateral solution, $CaCl_2$ was increased to 4 mM to compensate for the Ca^{2+}-chelating capacity of the gluconate (16).

Cyclic AMP Assay

Cellular cAMP was measured using an ELISA-based detection kit, as previously described (20). Briefly, cells grown on 60-mm dishes ($\sim 7 \times 10^6$ cells/dish) were stimulated with FP, budesonide (BUD), forskolin, or vehicle. The cells were then lysed in 0.1 N HCl for 20 to 30 minutes after treatment with these agents, and cAMP was measured. We determined the cytosolic cyclic AMP concentration $[cAMP]_i$ in the samples according to the manufacturer's instructions.

Analysis of Results

Numerical data are presented as means ± SD. Statistical differences were determined by the Student *t* test for comparisons of data between two groups, or one-way ANOVA for multiple group comparisons. $P < 0.05$ was considered statistically significant.

RESULTS

Effects of Fluticasone Propionate on Airway Anion Transport

The basal I_{SC} and transepithelial resistance in our experiments using Calu-3 cells were 11.7 ± 4.7 μA/cm^2 and 350.4 ± 80.1 Ωcm^2, respectively ($n = 84$). The cell monolayer immediately responded to the application of FP (100 μM) from the apical aspect, generating sustained I_{SC} (Figure 1A). The difference between the maximum and basal I_{SC} (ΔI_{SC}) was 9.2 ± 1.3 μA/cm^2 ($n = 5$). The fluticasone propionate–induced anion secretion was reduced

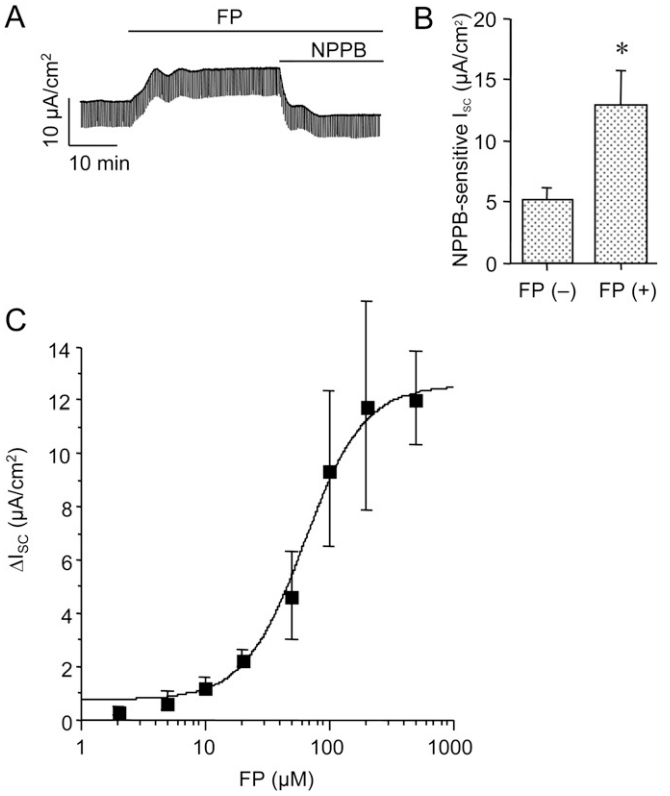

Figure 1. Representative traces of fluticasone dipropionate (FP) on short-circuit current (I_{sc}) response in Calu-3 cells. (*A*) The cell monolayer immediately responded to FP (100 μM) applied from the apical aspect, generating sustained I_{SC}. The FP-induced response was reduced by the application of 5′-nitro-2-(3-phenylpropylamino) benzoate (NPPB; 100 μM), a Cl^- channel blocker. (*B*) The NPPB-sensitive components in the FP-induced I_{SC} [FP (+)] were compared with those without FP [FP (−)]. (*C*) Increases in I_{SC} values in response to FP at various concentrations were measured. The maximum increases in I_{SC} from basal concentrations (i.e., I_{SC} values just before the addition of FP) are expressed as ΔI_{SC}. Data represent means ± SD ($n = 4$–5). *$P < 0.01$, significantly different from the values in the FP (−) groups.

by the application of NPPB (100 μM), a Cl^- channel blocker: the NPPB-sensitive component was 13.6 ± 2.8 μA/cm^2 ($n = 5$, $P < 0.01$), in comparison to that without FP (5.2 ± 0.9 μA/cm^2, $n = 5$; Figure 1B). To confirm the validity of 100 μM FP, we cumulatively added various concentrations of FP at intervals of approximately 5–10 minutes, because FP-induced I_{SC} responses reach a sustained state by 10 minutes, with the result that the ΔI_{SC} was increased in a concentration-dependent manner. The concentration for the half-maximal effect was 61.9 ± 1.5 μM ($n = 4$; Figure 1C).

Compared with the I_{SC} responses of the control sample to FP (Figure 2A), those in the presence of cAMP-related inhibitors (Figures 2B and 2C) were significantly suppressed. Namely, the FP-induced I_{SC} ($\Delta I_{SC} = 9.0 \pm 2.0$ μA/cm^2, $n = 5$) was reduced to 2.1 ± 1.0 μA/cm^2 ($n = 5$, $P < 0.01$) and 0.8 ± 0.5 μA/cm^2 ($n = 5$, $P < 0.01$) by the presence of the protein kinase A (PKA) inhibitor H89 (10 μM) and the adenylate cyclase inhibitor SQ22536 (100 μM), respectively (Figure 2D).

Effects of Fluticasone Propionate on Apical and Basolateral Anion Transporters

Anion secretion in Calu-3 cells is the product of coordinated activities of anion transporters on the apical and basolateral

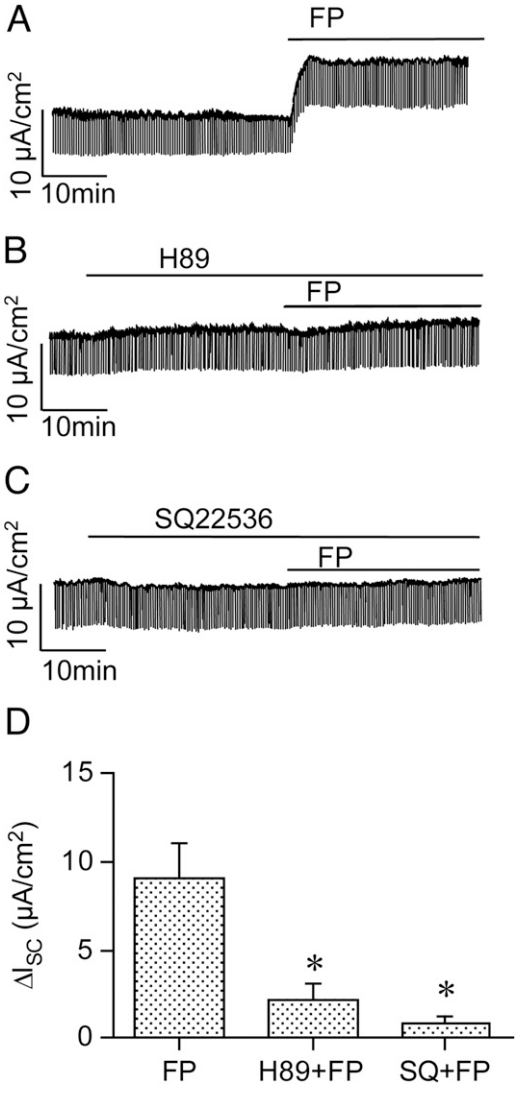

Figure 2. Pharmacological characterizations of short-circuit current (I_{SC}) in response to fluticasone dipropionate (FP) in Calu-3 cells. I_{SC} responses to FP (100 μM, apical) in the control sample (*A*) were compared with those in the presence of H89 (*B*) (10 μM, a protein kinase A inhibitor), and 9-tetrahydro-2-furyl-adenine (*C*) (SQ22536; 100 μM, an adenylate cyclase inhibitor). (*D*) A summary of the FP-induced I_{SC} increases (ΔI_{SC}) obtained from *A* (FP), *B* (H89 + FP), and *C* (SQ + FP). Data represent means ± SD ($n = 5$). *$P < 0.01$, significantly different from the values under the conditions without the inhibitors.

membranes (16). In the cells, basolateral anion uptake is regulated by several anion transporters, including the bumetanide-sensitive Na^+–K^+–$2Cl^-$ cotransporter NKCC1 (21), the DNDS-sensitive Na^+–$2HCO_3^-$ cotransporter NBC1 (22), and the DNDS-sensitive HCO_3^-/Cl^- exchanger AE2 (23). The HCO_3^- and Cl^- taken up by the cells commonly pass through the CFTR, a cAMP-regulated anion channel, in Calu-3 cells (16). Because basolateral anion entry is generally the rate-limiting step for transepithelial anion transport (24), we estimated the functions of basolateral anion transporters by measuring bumetanide (50 μM)–sensitive and DNDS (2 mM)–sensitive components in the FP-induced I_{SC}. As shown in Figure 3A, both components comprise the FP-induced I_{SC} (Figure 3A). Compared with the control sample, the former and latter components were increased, from 0.9 ± 0.7 μA/cm² ($n = 6$) and 1.0 ± 0.2 μA/cm² ($n = 6$) to 5.0 ± 1.5 μA/cm² ($n = 6$, $P < 0.01$) and 4.6 ± 1.1 μA/cm² ($n = 6$, $P < 0.01$), respectively (Figures 3B and 3C). On the other hand, apical Cl^- export was estimated as I_{Cl} in the nystatin-permeabilized monolayer in Figures 3D and 3E. Correlated with I_{SC} changes, the application of FP (100 μM) caused the development of an inward I_{Cl} ($\Delta I_{Cl} = 11.6 \pm 4.5$ μA/cm² at 20 minutes after its addition, $n = 6$; Figures 3D and 3F). The increases in the FP-induced I_{Cl} were counteracted by pretreatment with NPPB (100 μM), inhibitors of CFTR ($\Delta I_{Cl} = 1.5 \pm 0.9$ μA/cm², $n = 6$, $P < 0.01$; Figures 3E and 3F).

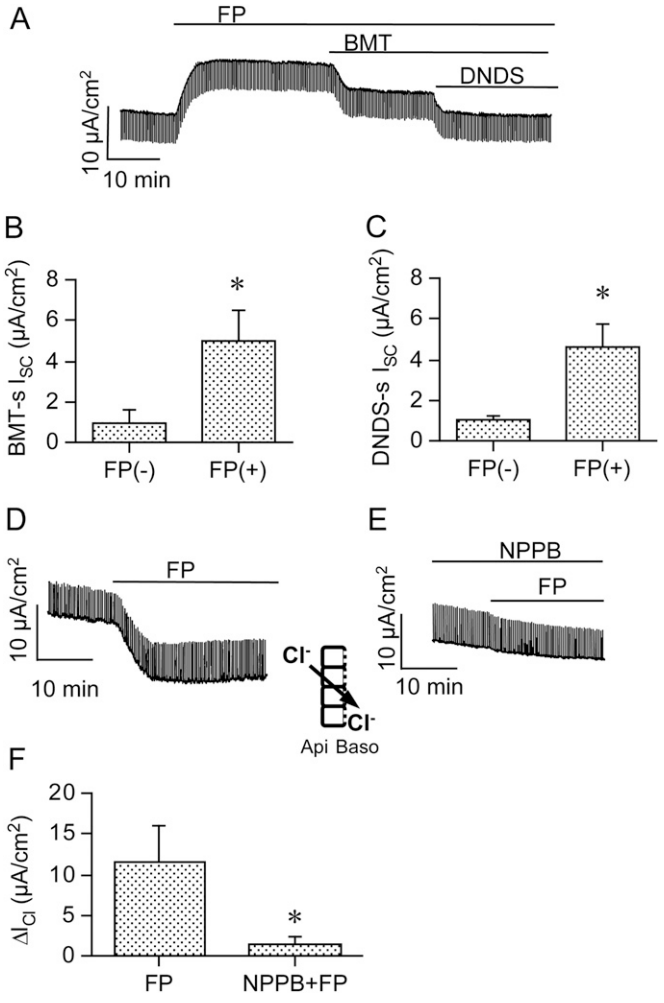

Figure 3. Functional analyses of fluticasone dipropionate (FP)–activated anion transporters on the basolateral and apical membrane. (*A*) FP-induced I_{SC} was reduced by the application of bumetanide (BMT, 50 μM, basolateral) and 4,4′-dinitrostilbene-2,2′-disulfonic acid (DNDS, 2 mM, basolateral). (*B* and *C*) Bumetanide-sensitive and DNDS-sensitive components in the I_{SC} (expressed as BMT-s and DNDS-s I_{SC}, respectively), with and without the application of 100 μM FP, are shown as FP (+) and FP (−), respectively. (*D* and *E*) Representative traces of changes in apical Cl^- conductance, estimated as I_{Cl} in the absence and presence of NPPB (100 μM, an effective CFTR blocker), respectively. The I_{Cl} currents were measured after the establishment of an apical–basolateral Cl^- gradient and permeabilization of the basolateral membrane with nystatin (100 μM, for more than 20 min). A downward I_{Cl} indicates an inward Cl^- current. (*F*) A summary of the values of FP-induced I_{Cl} increases (ΔI_{Cl}) obtained from *D* (FP) and *E* (NPPB + FP). Data represent means ± SD ($n = 6$). Significant differences are expressed as *$P < 0.01$ (unpaired Student *t* test). CFTR, cystic fibrosis transmembrane conductance regulator.

Bioelectric Interactions between FP and Forskolin-Stimulated Responses

cAMP-related stimuli are well-known to generate I_{SC} augmentations that reflect electrogenic anion transport. Indeed, the application of forskolin (10 μM, an adenylate cyclase activator; Figure 4A) to the basolateral face led to a rapid increase in I_{SC}, followed by a sustained component that is inhibited by bumetanide and DNDS. Figure 4B shows that the forskolin-induced increases in I_{SC} were attenuated by the presence of FP (100 μM). The forskolin-induced I_{SC} increases (ΔI_{SC}) were diminished from 52.5 ± 5.0 μA/cm^2 ($n = 6$) to 20.3 ± 4.3 μA/cm^2 ($n = 6$, $P < 0.01$) in the peak component, and from 21.9 ± 3.0 μA/cm^2 ($n = 6$) to 8.7 ± 2.4 μA/cm^2 ($n = 6$, $P < 0.01$) in the sustained component when both of them were estimated as increases from the I_{SC} concentrations just before the application of forskolin. When they are estimated as increases from basal I_{SC} concentrations before the application of FP, however, the sustained ΔI_{SC} values in the absence of FP were not significantly different from those in its presence (Figures 4B; ΔI_{SC} = 19.3 ± 4.9 μA/cm^2). Indeed, the bumetanide-sensitive and DNDS-sensitive components (7.9 ± 2.3 μA/cm^2 and 8.4 ± 2.0 μA/cm^2, $n = 6$, respectively) in the sustained I_{SC} in the experiments shown in Figure 4A were not significantly different from those in the experiments shown in Figure 4B (7.6 ± 1.9 μA/cm^2 and 9.0 ± 1.7 μA/cm^2, $n = 6$, respectively). In the nystatin-permeabilized monolayer used for the estimation of apical Cl^- conductance, FP-induced I_{Cl} increases under the forskolin-stimulated condition were markedly suppressed (2.1 ± 0.7 μA/cm^2, $n = 6$; Figure 4C), compared with those under the forskolin-unstimulated condition (11.2 ± 3.8 μA/cm^2, $n = 6$; Figure 4D). In the presence of FP (100 μM; Figure 4D), the I_{Cl} increases attributable to the application of forskolin were attenuated. The forskolin-induced I_{Cl} increases (ΔI_{Cl}) were suppressed to 10.6 ± 2.3 μA/cm^2 ($n = 6$, $P < 0.01$), compared with those in the absence of FP (21.0 ± 5.0 μA/cm^2, $n = 6$). However, the values were not significantly different from total I_{Cl} developments attributable to the combination of FP and forskolin that were estimated as increases from basal concentrations (21.9 ± 4.2 μA/cm^2, $n = 6$).

BUD Reproduced the Effects of Fluticasone Propionate

Figure 5A shows representative traces of BUD (100 μM)–induced I_{SC} (ΔI_{SC} = 6.2 ± 2.8 μA/cm^2, $n = 5$). Like the effects of FP, the bumetanide-sensitive and DNDS-sensitive I_{SC} (0.9 ± 0.3 μA/cm^2, $n = 5$, and 1.0 ± 0.5 μA/cm^2, $n = 5$, respectively) were significantly increased to 2.8 ± 1.0 μA/cm^2 ($n = 5$) and 3.5 ± 1.2 μA/cm^2 ($n = 5$, $P < 0.01$), respectively, by the application of BUD (Figures 5B and 5C). Apical Cl^- export was estimated as I_{Cl} in the nystatin-permeabilized monolayer in Figures 5D and 5E. Under the forskolin-unstimulated condition, the application of BUD (100 μM) caused the development of an inward I_{Cl} (ΔI_{Cl} = 6.1 ± 2.2 μA/cm^2, $n = 4$; Figure 5D). Compared with the response, BUD-induced I_{Cl} increases under the forskolin-stimulated condition were markedly suppressed (ΔI_{Cl} = 1.9 ± 0.7 μA/cm^2, $n = 4$, $P < 0.05$; Figure 5E).

Effects of FP and BUD on Cytosolic cAMP Concentrations

In the cytosolic cAMP assay (Figure 6), applications of FP for 30 minutes did not cause significant changes in $[cAMP]_i$ (3.5 ± 1.4 pmol/10^6 cells, $n = 6$), compared with the control sample (4.0 ± 1.7 pmol/10^6 cells, $n = 6$), despite the I_{SC} and I_{Cl} changes. Nor did BUD applications cause significant changes in basal $[cAMP]_i$ (4.0 ± 1.3 pmol/10^6 cells, $n = 6$). Forskolin stimulation for 20 minutes increased $[cAMP]_i$ to 54.8 ± 7.9 pmol/10^6 cells, whereas the presence of FP and BUD potentiated the effects of forskolin, increasing $[cAMP]_i$ concentrations further to 160.3 ± 14.3 pmol/10^6 cells ($n = 6$, $P < 0.01$) and 141.6 ± 25.4 pmol/10^6 cells ($n = 6$, $P < 0.01$), respectively. In addition, a similar synergism was observed in the effects of another inhaled corticosteroid, beclomethasone dipropionate (100 μM), under the same conditions (164.3 ± 18.0 pmol/10^6 cells, $n = 6$, $P < 0.01$).

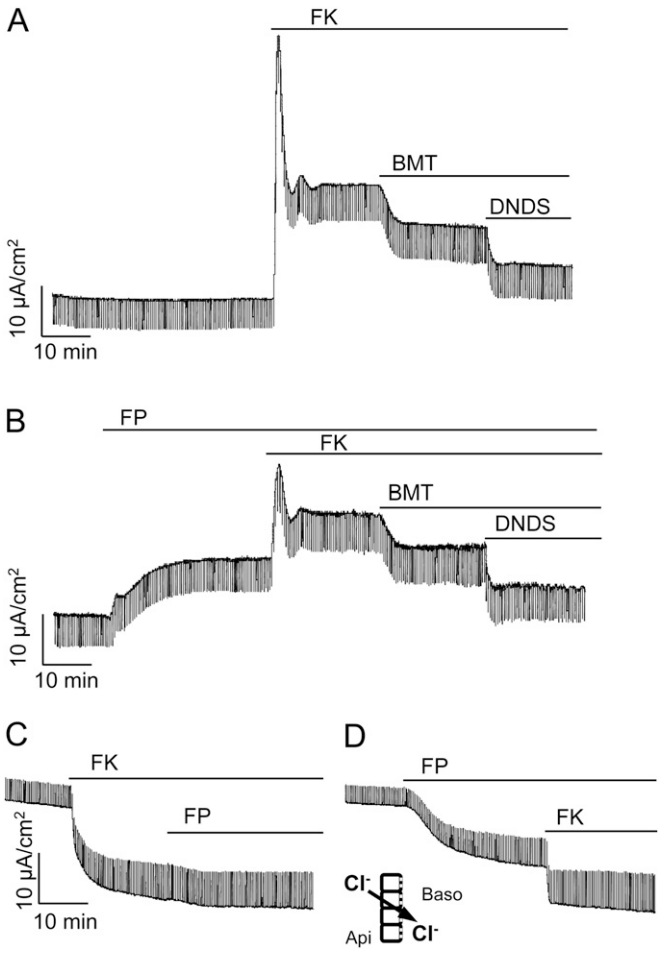

Figure 4. Bioelectric interactions between fluticasone propionate (FP)–stimulated and forskolin (FK)–stimulated responses. (*A*) Representative traces of I_{SC} in response to FK (10 μM) for the control sample. (*B*) Representative traces of FK-induced I_{SC} in the presence of FP (100 μM). (*C* and *D*) Representative traces of the FP (100 μM)–induced I_{Cl} in the presence of FK (10 μM, *C*) and FK-induced I_{Cl} in the presence of FP (100 μM, *D*), respectively. The I_{Cl} currents were estimated after the establishment of an apical–basolateral Cl^- gradient and permeabilization of the basolateral membrane with nystatin (100 μM, for more than 20 min). A downward I_{Cl} indicates an inward Cl^- current.

DISCUSSION

The local delivery of inhaled corticosteroids may yield considerably higher concentrations on the airway surface. FP is considered to be slowly absorbed over a long period of time after deposition in the lungs (25). The total lung deposition of radiolabeled FP administered with a metered dose inhaler has been shown to range from 10–36% (22% ± 9%) in adults (26). To determine the average concentration of a drug on the airway surface after its deposition, it is necessary to know the volume of the airway surface liquid. Widdicombe (27) estimated that the liquid volumes are 1.0 ml for the trachea and bronchi, and

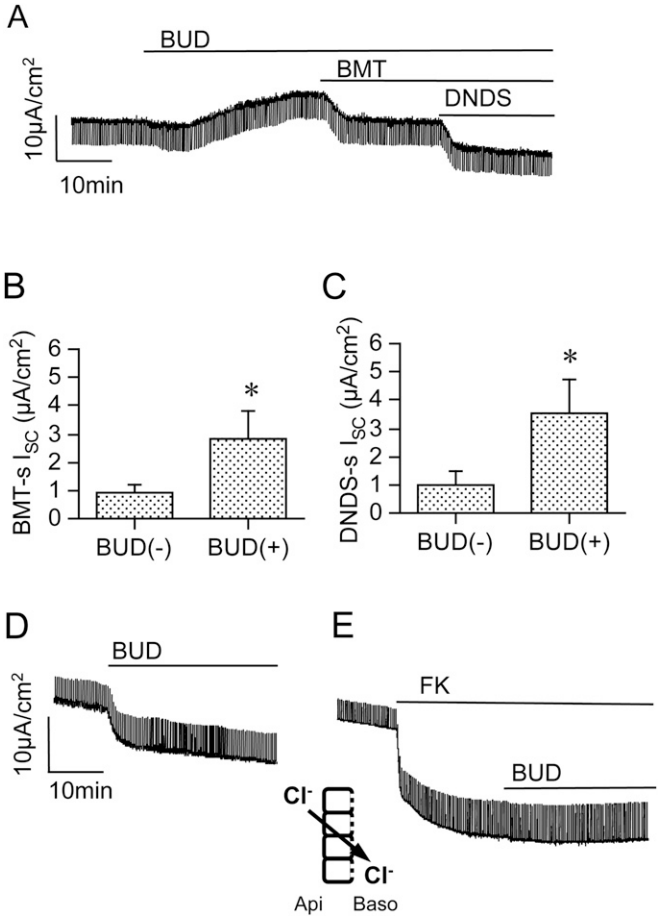

Figure 5. I_{SC} and I_{Cl} responses to budesonide (BUD, 100 μM) in Calu-3 cells. (*A*) The BUD-induced I_{SC} was reduced by the application of bumetanide (BMT, 50 μM, basolateral) and DNDS (2 mM, basolateral). (*B* and *C*) BMT-sensitive and DNDS-sensitive components in the I_{SC} (expressed as BMT-s and DNDS-s I_{SC}, respectively) under the basal condition [BUD (−)], and those components after stimulation with BUD [BUD (+)], respectively. *Significant differences are expressed as $P < 0.01$ ($n = 5$). (*D* and *E*) representative traces of the BUD (100 μM)–induced I_{Cl} in the absence and presence of forskolin (FK, 10 μM) in the monolayer permeabilized with a basolateral application of nystatin (100 μM). (*D*) The application of BUD from the apical aspect stimulated inward sustained I_{Cl}. (*E*) Under the forskolin-stimulated condition, the effect of BUD suppressed the change in I_{Cl}.

2.6 ml for the conducting bronchioles. Combining these lines of information indicates that inhaling FP (molecular weight, 500.57) at 800 μg (1.6 μmol) by mouth would result in the average concentration on the airway surface as follows: airway surface FP = 1.6 μmol × 0.22 (% lung deposition)/(1.0 + 2.6) ml = 98 μM.

However, the deposition of inhaled FP in the airways is uneven (28), and FP is predominantly deposited in the proximal respiratory tract (29). Based on this conjecture, we applied FP at 100 μM to the airway epithelial cells, resulting in immediate rises of I_{SC}, followed by sustained currents. The FP-induced responses were inhibited by the presence of NPPB (a Cl^- channel blocker), bumetanide (an inhibitor of the NKCC1 Na^+–K^+–$2Cl^-$ cotransporter), or DNDS (an inhibitor of the NBC1/AE2 HCO_3^-–dependent anion transporter), suggesting that the FP-induced responses are composed of anion secretion. The concentration for the half-maximal effect was approximately 60 μM, which is possibly within the range of the clinically used concentration.

In general, cAMP/PKA is a key molecule for anion secretion in any polarized epithelial cell, including Calu-3 submucosal gland cells (30). In the present study, we showed that the FP-induced I_{SC} were significantly reduced by the presence of inhibitors of PKA and adenylate cyclase. We also found that FP stimulated I_{Cl}, reflecting activation of the cAMP-dependent Cl^- channel CFTR, which is the exclusive gate for Cl^- export in Calu-3 cells (18). These results indicate that the nongenomic effects of FP, at least in part, involve cAMP-dependent cascades to stimulate gland secretion.

As shown in our additional data (*see* Figure E1 in the online supplement), however, FP-induced Cl^- secretion was not evoked in normal human bronchial epithelial cells, which show Na^+ absorption but much less CFTR-mediated Cl^- secretion. Moreover, Na^+ absorption was not affected by FP in the cells. Thus, FP may exert its nongenomic effects on gland secretion in particular, to enhance mucociliary clearance in the respiratory tract.

As shown in the present study, the forskolin-induced and FP-induced I_{SC} were composed of rapid increases and subsequent sustained increases, as demonstrated in previous studies using cAMP-related agents (16, 31). Especially in the forskolin-induced responses, the sustained levels were much lower than the initial peak points (Figure 4A). However, the peak components were not detected in the changes of apical membrane Cl^- conductance in the nystatin-permeabilized monolayer (Figure 4C). In general, cAMP-dependent anion secretion is characterized not only by apical CFTR activation, but also by the parallel activation of NKCC1 and NBC1/AE2 anion transporters (15, 20) Thus, it is conceivable that (*1*) the initial phase is produced by a gush of anions that had accumulated in the cells beforehand, and (*2*) the sustained phase is maintained by the function of basolateral anion transporters such as NKCC1, NBC1, and AE2. During anion transport, however, the cAMP-dependent

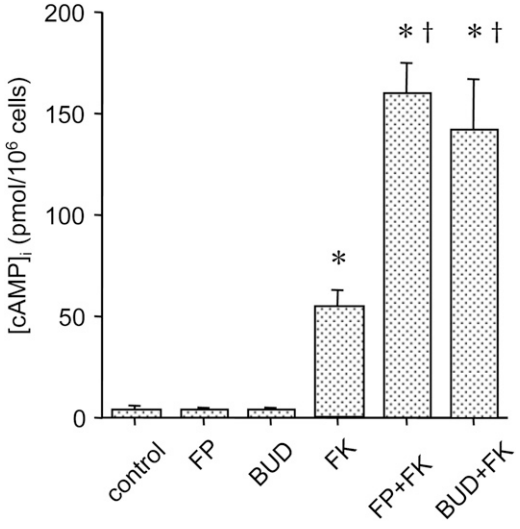

Figure 6. Effects of inhaled corticosteroids on changes in cytosolic cAMP concentrations ($[cAMP]_i$) in the forskolin (FK)–unstimulated and FK-stimulated groups. In the former groups, the measurements were performed 30 minutes after the addition of fluticasone dipropionate (FP, 100 μM), budesonide (BUD, 100 μM), and or its vehicle (0.05% DMSO, control). In the latter, the monolayer was exposed to FK for 20 minutes after a 30-minute pretreatment with FP or BUD. Data represent means ± SD ($n = 6$). *$P < 0.01$ and †$P < 0.01$ indicate significant differences from the values of FK-unstimulated (shown as "control") and FK-stimulated control groups (shown as "FK"), respectively.

regulation of NKCC1 is indirect and is attributable to the secondary effects of cAMP on changes in cell volume, the cytoskeleton, and intracellular Cl^- concentrations, leading to the regulation of various kinases, including protein kinase C (32, 33).

We also showed that stimulation by FP failed to enhance the I_{SC} and I_{Cl} responses to forskolin, namely, (*1*) bumetanide-sensitive and DNDS-sensitive components in the forskolin-stimulated I_{SC} were not significantly increased by the presence of FP, and (*2*) forskolin-induced I_{Cl} was less up-regulated by FP. These observations suggest that FP and forskolin share elements of a common signaling pathway for the activation of CFTR, NKCC1, NBC1, and AE2.

In the cytosolic cAMP assay, however, we found that FP synergistically increased $[cAMP]_i$ in combination with forskolin. Similar results were obtained by using a combination of FP and the β-adrenergic receptor (β_2-AR) agonist salmeterol, which are currently used as a standard combination therapy for patients with asthma (*see* Figure E2 in the online supplement). Thus, FP is likely to exert its effects on adenylate cyclase without competing with the conventional pathway for the activation of adenylate cyclase by means of forskolin or β_2-AR stimulation. However, our results of no significant effects of FP on $[cAMP]_i$ in the absence of forskolin do not necessarily negate the involvement of cAMP in the effects of FP. A signaling pathway to activate an apical adenylate cyclase closely associated with CFTR in Calu-3 cells has been proposed (34). Like the inhaled corticosteroids, cAMP/PKA-related agents such as phosphodiesterase inhibitors and adenosine also stimulate Cl^- secretion in the setting of very low or often undetectable [cAMP]i concentrations (31, 35). In general, these observations have been also interpreted as the results of compartmentalized changes in cAMP concentrations in the subcellular region (34, 36).

In the present study, we demonstrated that BUD reproduced the effects of FP on I_{SC}, I_{Cl}, and $[cAMP]_i$. Beclomethasone dipropionate also potentiated $[cAMP]_i$ in the presence of forskolin, and it caused similar but smaller effects in I_{SC} (data not shown). This suggests that the nongenomic effects of inhaled corticosteroids share a common mechanism.

In Calu-3 cells, cAMP stimulation induces the parallel activation of NKCC1 and NBC1/AE2, as did FP and BUD, whereas Ca^{2+}-mediated stimuli generate the selective up-regulation of NKCC1 (15, 16, 20, 37). Although the Ca^{2+}-induced Cl^- secretion is inhibited by charybdotoxin, a selective KCNN4 Ca^{2+}-activated K^+ channel blocker (30), neither FP-induced nor BUD-induced responses were sensitive to charybdotoxin (data not shown). This indicates less of a contribution of Ca^{2+}-mediated mechanisms to the nongenomic effects of FP and BUD.

Taken together, inhaled corticosteroids such as FP and BUD stimulate CFTR-mediated anion transport through adenylate-cyclase–mediated mechanisms in a nongenomic fashion, thus sharing elements of a common signaling pathway for the activation of cAMP-activated anion transporters (e.g., CFTR) with other cAMP-related stimuli. However, the combination of corticosteroids with forskolin induces the synergistic production of cAMP, suggesting that corticosteroids and forskolin have different target sites on adenylate cyclase. Figure 7 constitutes a schematic drawing of the hypothetical mechanism, taking the effects of FP on the CFTR as an example. Likewise, the combination of FP and a β_2-AR agonist salmeterol synergistically increases cytosolic cAMP concentrations. Thus, FP/salmeterol combination therapies, which are currently used for bronchial asthma and chronic obstructive pulmonary disease, may comprise more rational treatments than previously thought. The nongenomic effects of these agents may involve therapeutic aspects for mucus congestive airway diseases, in addition to their genomic effects that are generally recognized.

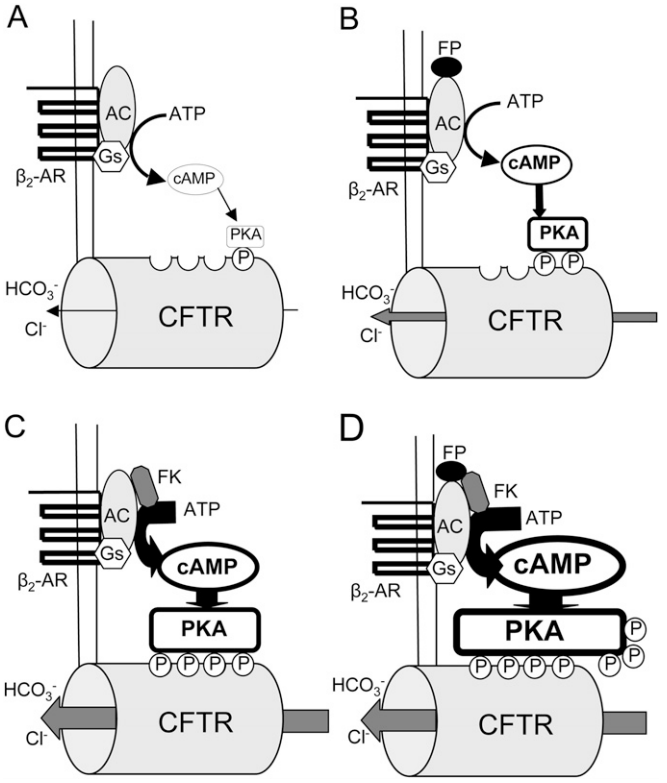

Figure 7. Hypothetical models of the mechanisms underlying the effects of fluticasone dipropionate (FP) on the CFTR, a cAMP-activated Cl^-/HCO_3^- channel on the apical membrane. (*A*) Basal activities of CFTR are maintained by basal protein kinase A (PKA)–mediated phosphorylation. (*B*) FP stimulates the cAMP-signaling pathway from adenylate cyclase (AC) to CFTR in the subcellular region. In the process, locally generated cAMP to activate CFTR is at undetectable [cAMP]i concentrations. (*C*) The stimulation of AC by forskolin (FK) or G_s-protein–coupled β_2-adrenergic receptor (β_2-AR) activated the CFTR, with detectable increases in $[cAMP]_i$. (*D*) The effects of FP on AC synergistically enhanced cAMP production, in combination with these cAMP-related agents. FP exerts its effect on AC without competing with the conventional pathway for AC activation.

Author disclosures are available with the text of this article at www.atsjournals.org.

References

1. Barnes PJ. Inhaled glucocorticoids: new developments relevant to updating of the asthma management guidelines. *Respir Med* 1996;90:379–384.
2. Brogden RN, Heel RC, Speight TM, Avery GS. Beclomethasone dipropionate: a reappraisal of its pharmacodynamic properties and therapeutic efficacy after a decade of use in asthma and rhinitis. *Drugs* 1984;28:99–126.
3. Brogden RN, McTavish D. Budesonide: an updated review of its pharmacological properties, and therapeutic efficacy in asthma and rhinitis. *Drugs* 1992;44:375–407.
4. Purucker ME, Rosebraugh CJ, Zhou F, Meyer RJ. Inhaled fluticasone propionate by diskus in the treatment of asthma: a comparison of the efficacy of the same nominal dose given either once or twice a day. *Chest* 2003;124:1584–1593.
5. Barnes PJ. Corticosteroid effects on cell signalling. *Eur Respir J* 2006;27:413–426.
6. Falkenstein E, Tillmann HC, Christ M, Feuring M, Wehling M. Multiple actions of steroid hormones: a focus on rapid, nongenomic effects. *Pharmacol Rev* 2000;52:513–556.
7. White RE, Darkow DJ, Lang JL. Estrogen relaxes coronary arteries by opening BKCa channels through a cGMP-dependent mechanism. *Circ Res* 1995;77:936–942.

8. Liu XK, Katchman A, Ebert SN, Woosley RL. The antiestrogen tamoxifen blocks the delayed rectifier potassium current, IKr, in rabbit ventricular myocytes. *J Pharmacol Exp Ther* 1998;287:877–883.
9. Nakajima T, Kitazawa T, Hamada E, Hazama H, Omata M, Kurachi Y. 17beta-estradiol inhibits the voltage-dependent L-type Ca^{2+} currents in aortic smooth muscle cells. *Eur J Pharmacol* 1995;294:625–635.
10. Ruehlmann DO, Steinert JR, Valverde MA, Jacob R, Mann GE. Environmental estrogenic pollutants induce acute vascular relaxation by inhibiting L-type Ca^{2+} channels in smooth muscle cells. *FASEB J* 1998;12:613–619.
11. Valverde MA, Mintenig GM, Sepulveda FV. Differential effects of tamoxifen and I^- on three distinguishable chloride currents activated in T84 intestinal cells. *Pflugers Arch* 1993;425:552–554.
12. Zhang JJ, Jacob TJ, Valverde MA, Hardy SP, Mintenig GM, Sepulveda FV, Gill DR, Hyde SC, Trezise AE, Higgins CF. Tamoxifen blocks chloride channels: a possible mechanism for cataract formation. *J Clin Invest* 1994;94:1690–1697.
13. Quinton PM. Cystic fibrosis: righting the wrong protein. *Nature* 1990;347: 226.
14. Shen BQ, Finkbeiner WE, Wine JJ, Mrsny RJ, Widdicombe JH. Calu-3: a human airway epithelial cell line that shows cAMP-dependent Cl^- secretion. *Am J Physiol* 1994;266:L493–L501.
15. Hibino Y, Morise M, Ito Y, Mizutani T, Matsuno T, Ito S, Hashimoto N, Sato M, Kondo M, Imaizumi K, *et al*. Capsaicinoids regulate airway anion transporters through Rho kinase– and cyclic AMP–dependent mechanisms. *Am J Respir Cell Mol Biol* 2011;45:684–691.
16. Devor DC, Singh AK, Lambert LC, DeLuca A, Frizzell RA, Bridges RJ. Bicarbonate and chloride secretion in Calu-3 human airway epithelial cells. *J Gen Physiol* 1999;113:743–760.
17. Son M, Ito Y, Sato S, Ishikawa T, Kondo M, Nakayama S, Shimokata K, Kume H. Apical and basolateral ATP-induced anion secretion in polarized human airway epithelia. *Am J Respir Cell Mol Biol* 2004;30: 411–419.
18. Haws C, Finkbeiner WE, Widdicombe JH, Wine JJ. CFTR in Calu-3 human airway cells: channel properties and role in cAMP-activated Cl^- conductance. *Am J Physiol* 1994;266:L502–L512.
19. Wine JJ, Finkbeiner WE, Haws C, Krouse ME, Moon S, Widdicombe JH, Xia Y. CFTR and other Cl^- channels in human airway cells. *Jpn J Physiol* 1994;44:S199–S205.
20. Morise M, Ito Y, Matsuno T, Hibino Y, Mizutani T, Ito S, Hashimoto N, Kondo M, Imaizumi K, Hasegawa Y. Heterologous regulation of anion transporters by menthol in human airway epithelial cells. *Eur J Pharmacol* 2010;635:204–211.
21. Liedtke CM, Hubbard M, Wang X. Stability of actin cytoskeleton and PKC-delta binding to actin regulate NKCC1 function in airway epithelial cells. *Am J Physiol Lung Cell Mol Physiol* 2003;284:C487–C496.
22. Inglis SK, Finlay L, Ramminger SJ, Richard K, Ward MR, Wilson SM, Olver RE. Regulation of intracellular pH in Calu-3 human airway cells. *J Physiol* 2002;538:527–539.
23. Loffing J, Moyer BD, Reynolds D, Shmukler BE, Alper SL, Stanton BA. Functional and molecular characterization of an anion exchanger in airway serous epithelial cells. *Am J Physiol Cell Physiol* 2000;279: C1016–C1023.
24. Matthews JB. Molecular regulation of Na^+–K^+–$2Cl^-$ cotransporter (NKCC1) and epithelial chloride secretion. *World J Surg* 2002;26:826–830.
25. Esmailpour N, Hogger P, Rabe KF, Heitmann U, Nakashima M, Rohdewald P. Distribution of inhaled fluticasone propionate between human lung tissue and serum *in vivo*. *Eur Respir J* 1997;10:1496–1499.
26. Leach CL, Davidson PJ, Hasselquist BE, Boudreau RJ. Lung deposition of hydrofluoroalkane-134a beclomethasone is greater than that of chlorofluorocarbon fluticasone and chlorofluorocarbon beclomethasone: a cross-over study in healthy volunteers. *Chest* 2002;122:510–516.
27. Widdicombe JH. Volume of airway surface liquid in health and disease. *Am J Respir Crit Care Med* 2002;165:1566.
28. Leach CL, Davidson PJ, Boudreau RJ. Improved airway targeting with the CFC-free HFA-beclomethasone metered-dose inhaler compared with CFC-beclomethasone. *Eur Respir J* 1998;12:1346–1353.
29. Burgel PR, de Blic J, Chanez P, Delacourt C, Devillier P, Didier A, Dubus JC, Frachon I, Garcia G, Humbert M, *et al*. Update on the roles of distal airways in asthma. *Eur Respir Rev* 2009;18:80–95.
30. Moon S, Singh M, Krouse ME, Wine JJ. Calcium-stimulated Cl^- secretion in Calu-3 human airway cells requires CFTR. *Am J Physiol* 1997;273:L1208–L1219.
31. Cobb BR, Fan L, Kovacs TE, Sorscher EJ, Clancy JP. Adenosine receptors and phosphodiesterase inhibitors stimulate Cl^- secretion in Calu-3 cells. *Am J Respir Cell Mol Biol* 2003;29:410–418.
32. Liedtke CM, Papay R, Cole TS. Modulation of Na–K–2Cl cotransport by intracellular Cl^- and protein kinase C–delta in Calu-3 cells. *Am J Physiol Lung Cell Mol Physiol* 2002;282:L1151–L1159.
33. Lytle C, McManus T. Coordinate modulation of Na–K–2Cl cotransport and K–Cl cotransport by cell volume and chloride. *Am J Physiol Cell Physiol* 2002;283:C1422–C1431.
34. Huang P, Lazarowski ER, Tarran R, Milgram SL, Boucher RC, Stutts MJ. Compartmentalized autocrine signaling to cystic fibrosis transmembrane conductance regulator at the apical membrane of airway epithelial cells. *Proc Natl Acad Sci USA* 2001;98:14120–14125.
35. Bulteau L, Dérand R, Mettey Y, Métayé T, Morris MR, McNeilly CM, Folli C, Galietta LJ, Zegarra-Moran O, Pereira MM, *et al*. Properties of CFTR activated by the xanthine derivative X-33 in human airway Calu-3 cells. *Am J Physiol Cell Physiol* 2000;279:C1925–C1937.
36. Fischer H, Schwarzer C, Illek B. Vitamin C controls the cystic fibrosis transmembrane conductance regulator chloride channel. *Proc Natl Acad Sci USA* 2004;101:3691–3696.
37. Cowley EA, Linsdell P. Characterization of basolateral K^+ channels underlying anion secretion in the human airway cell line Calu-3. *J Physiol* 2002;538:747–757.